Behavior Analysis of the Nonwoven Needle-Punched Polyester Fabrics Due to Compression Loading

Hasan Mashroteh*, Esfandiar Ekhtiyari, Saeed Fattahi, Ali Aflatounian, Hosein Rahimi, and Milad Sadeghi-Sadeghabad

Abstract- **This study investigates bursting strength, puncture resistance and the relevant real elongations of the nonwoven needle-punched polyester fabrics using compressive behavior study and statistical design of experiment known as three-factor factorial design. To evaluate effect of main parameters of fabric structure, seventy-five samples were prepared and a prediction model was developed by multiple linear regression method. The results unanimously showed that samples have undeniable similarities in the compression behavior, so that four distinguished regions can be considered through the path tracing of the force-deflection curves. Additionally, it was concluded that the puncture's self-socking position takes place in less magnitude of elongation in comparison to the similar position of bursting. Stress concentration in puncture causes that the fabric rupture was due to fiber breakage rather than its slippage. Whereas, the bursting ruptures of the fabric are further the result of fiber slippage. This is clearly due to geometry of ball-shaped device which is led to the relative uniformity of the quality of bursting loading.**

Keywords: **nonwoven needle-punched fabric, bursting, puncture, strength, real elongation**

I. INTRODUCTION

Various nonwoven technologies in general and needle-punching process as a bonding method of the fibrous assemblies in particular, have experienced one of the fastest financial growthsinthe world textile industry in the recent years. Among the various synthetic fibers used in the nonwoven needle-punched fabrics, the polyester fiber is extensively used not only in conventional end-uses, but also in industrial high-performance applications. This is due to the acceptable physical and mechanical properties of the polyester fiber, along with its economic aspects. It is clear that the majority of the nonwoven needle-punched polyester fabrics such as geotextiles, automotive floor-coverings and home/official furnishings, are subjected to compression loading either in the manufacturing process or in their applications. Additionally, the fabric deformations due to compression loading usually take place in the forms of bursting and puncture.

Dynamic puncture testing is based on a cone drop procedure [1]; but, tests of bursting and static puncture (CBR) are carried out by conventional strength tester. Whereas, the cone drop test merely reports diameter of the resultant hole as an indicator of the puncture resistance; strength tester measures both values of strength and deflection of the tested sample at break.

Bursting strength and static puncture resistance are in fact, the rupture forces which are compressively subjected to the fabric at a multi-directional loading using by perpendicular movement of a ball-shaped and a plunger-shaped body into the fabric respectively [2,3]. As a result, the shape of fabric deformation and consequently, real elongation of the fabric are totally different between bursting and static puncture tests; whereas, the strength tester may measure same value of deflection for the both tests due to equal displacement of the moving body into the fabric. Fig. 1 shows fabric deformations of bursting and static puncture, respectively in the statues of the quasi-Gaussian and quasi-hyperbolic. Therefore, this research aims to study strength and real elongation (not deflection) of the nonwoven needle-punched polyester fabrics, while they meet standard compression loading in the known forms of the bursting and static puncture.

Study of mechanical properties of the nonwoven needle-punched fabrics comes back to 60's, when the researchers tried to investigate effect of material, needling parameters and basis weight [5-7].

Then, Watanabe, Miwa, Yokoi, and Nakayama studied the effect of punch density on mechanical characteristics of the aramid nonwoven fabrics during the hot-press fatigue cycling process [8]. They found that a nonwoven fabric with higher value of punch density has a small

H. Mashroteh, E. Ekhtiyari, S. Fattahi, A. Aflatounian, H. Rahimi, and M. Sadeghi-Adeghabad
Department of Textile Engineering, Yazd University, 89168-69511 Yazd, Iran.

Correspondence should be addressed to H. Mashroteh
e-mail: mashroteh@yazd.ac.ir

(a) (b)

Fig. 1. Fabric deformation resulted by compression loading: (a) the quasi-gaussian status for bursting and (b) the quasi-hyperbola status for static puncture (CBR).

compressive strain and a high compressive modulus. This means that it is stiffer. They also indicated that after hot-press fatigue loading, changes in tensile and compressive behaviors are closely related to structural packing density of the nonwoven fabric. In addition to the researchers who focused on the compression resilience of the acrylic, jute-polypropylene and polyester nonwoven needle-punched fabrics [9-12], several studies reported changes in dimensional and mechanical properties of the polyester geotextile nonwoven fabrics based on the investigation of the various production parameters [13-15]. They showed that the performance of the geotextile samples was hardly affected by the pore size of the fabrics; especially, when the fabric is subjected to a compression loading.

S. Ghosh and Chapman studied molding formation of polyester/nylon blended nonwoven needle-punched fabrics with consideration of weight proportions and needling parameters [16]. They indicated that increment of the nylon weight-fraction to a given percentage causes to the increase of heated bursting strength. More needle-punched density and needle penetration depth more heated bursting strength, they also revealed. E. Koç and E. Çinçik analyzed the bursting strength of the short staple polyester/viscose needled-punched nonwoven fabrics [17]. The predicted regression model indicated that the bursting strength of the samples initially decreases and then increases with the enhancement of polyester fiber percentage. The model also showed that though, mass per unit area has a direct effect; but, when the arealweight is kept constant, increase in punch density causes the bursting strength to decrease. Das and Raghav investigated the bursting behavior of various polypropylene heat-sealed spun-bond nonwoven fabrics under different pressure conditions and basis weights [18,19]. They also studied other properties of the fabrics such as tensile characteristics and air permeability after cyclic bursting compression.

T.K. Ghosh evaluated puncture resistance of woven and nonwoven polypropylene geotextile fabrics under uniform radial pre-strain [20]. He observed lower failure strain, while the tested sample was pre-strained. Termonia developed a geometrical model for study of the factors controlling resistance of fibrous structures against needle puncture [21]. The results revealed that the puncture behavior occurs in four different stages during the needle displacement: (i) contact pressure of the tip of the needle against a fiber strand, leading to a steady increase in force; (ii) slippage of the tip into inter-fiber spacing, resulting to a sharp reduction of force; (iii) friction of the conical section of the needle against the fabric, leading to resumption of the force incrementand finally, and (iv) slippage of the conical section through the fabric, resulting in a steady decrease in force. Rawal, Anand, and Shah reported that the web area density has a significant effect on the puncture resistance of PP needle-punched nonwoven fabrics, whereas influence of the needle penetration depth is negligible [14]. They also found that the effect of punch density is more significant in comparison to that of needle penetration depth. Fangueiro, Carvalho, and Soutinho investigated that the puncture resistance increases with enhancement of the areal weight of the PP/PES/PAC nonwoven fabric [22]. Askari, Najar, and Vaghasloo researched on the effect of penetration speed and area unit weight of fabric on the puncture behavior of polyester needle-punched nonwoven geotextile fabrics using CBR test [23]. They indicated that the fabric areal weight significantly influences puncture resistance as well as puncture energy and elongation, while penetration speed merely affects the fabric puncture resistance and the relevant energy. Various studies of puncture resistance have also been reported for composite nonwoven fabrics [24-29]. They showed different behaviors of puncture resistance in nonwoven/woven fabrics compounded by Kevlar, low-T_m/high-T_m polyester, PA6 materials, etc.

In the most of the previous studies, static puncture (mainly CBR) and bursting behaviors of the needle-punched nonwoven fabrics have been investigated in the terms of strength and deflection. But, any attention has been taken to the real elongation of the deformed fabric during the static puncture and bursting. Thus, this research firstly describes calculation of the real elongation of the burst and punctured fabric in a simple way based on value of deflection obtained by the universal strength tester. Then, it reports strength and real elongation of the tested fabrics to statistically predict significance level of the studied vital parameters of the fabrics such as basis weight, needle penetration depth and punch density, in addition to compressive behavior study.

II. EXPERIMENTAL

In this study, the bursting test was conducted by Shirley

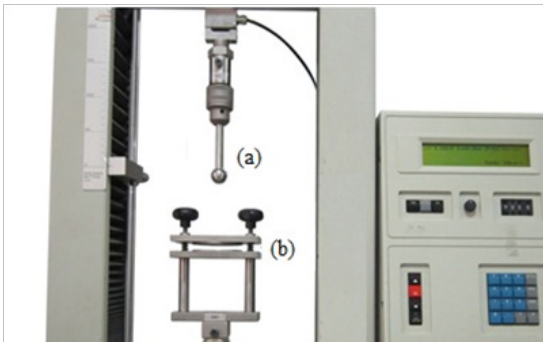

Fig. 2. Bursting device attached on the shirley universal tensile tester: (a) a ball-shaped device attached to the load cell and (b) clamping mechanism including two circular plates.

universal strength tester according to ASTM D6797-02 [2]. In this procedure, the tensile tester was equipped by a ring fabric clamping mechanism with internal diameter of 44.5 mm to hold the test specimen. A polished steel ball with diameter of 25.4 mm was also connected to the moveable member of the tensile tester. The compression speed was adjusted at constant rate of elongation of 305 mm/min. Two circular plates hold the sample of 80 mm×80 mm in dimensions, shown in Fig. 2.

The needle-punched nonwoven fabrics were also static puncture tested by the same strength tester, as shown in Fig. 3, based on ISO 12236 standard test method [3]. A stainless steel plunger with a diameter of 50 mm was fixed to the load cell which showed constant rate of movement at 50 mm/min. The tested samples were sized as 210×210 mm^2 and placed between two circular plates with a 150 mm diameter hole in the center.

Deflection value is a vertical deformation of the tested fabric measured by the strength tester; whereas, the fabric elongation refers to an extension which takes place at the surface plane of the fabric. As far as mechanical behavior of the nonwoven fabrics is concerned, the elongation parameter which describes quality of displacement of fibers

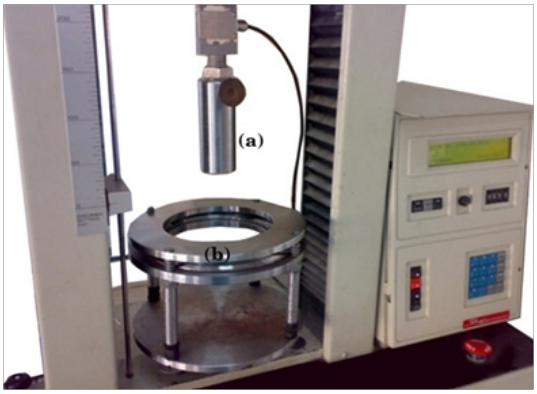

Fig. 3. Puncture device installed on the Shirley universal tensile tester: (a) a plunger device attached to the load cell and (b) clamping mechanism including two circular plates.

during loading is considered as a vital factor. It is clear that the real elongation magnitude of the tested fabric during bursting and puncture loadings can be easily calculated from the theoretical deformation geometry as shown in Fig. 4. Eqs. (1) and (2) indicate real elongation percentage of bursting (BRE) and puncture (PRE) at break, respectively.

$$BRE = \frac{\left(2\sqrt{(R_B - r_B)^2 + (h_B - r_B)^2} + \pi r_B) - 2R_B\right)}{2R_B} \times 100 \quad (1)$$

$$PRE = \frac{\left(2\sqrt{(R_P - r_P)^2 + h_P^2} + 2r_P) - 2R_P\right)}{2R_P} \times 100 \quad (2)$$

Where, r_B and r_p are radius of the ball device (12.7 mm) and the plunger device (25 mm), R_B and R_P are radius of the sample in the bursting (22.25 mm) and puncture (75 mm), and h_B and h_p are deflection value in the bursting and puncture (measured by the strength tester).

In this study, in order to investigate bursting and puncture behavior of nonwoven needle-punched fabrics, a statistical design of experiment known as three-factor factorial design was employed to evaluate the effect of independent studied variables. The models were also analyzed by multivariate regression method to predict response variables by the criterion values of R^2 and R^2_{adj}. The selected independent variables were fabric areal weight (X_1), needle penetration depth (X_2), and punch density (X_3). Hence, pursuant to the considered levels of the independent variables (Table I); seventy-five fabric samples were used, which can be seen in Table II.

To produce needle-punched nonwoven fabrics, 100% polyester fibers with average linear density of 11 dtex and 92 mm average length (which is customarily used in industrial applications such as automotive floor-covering and geotextile) were processed on a conventional carding machine. The carded web with average areal weight of 25 g/m^2 was fed to a horizontal cross folding unit. The folded batt was fed to a pair of needle looms, needling from top and bottom, respectively. The both looms were equipped with GROZ-BECKERT barbed needles coded as 15*18*32*3R333G1002 [30]. The response variables were considered main parameters such as bursting strength

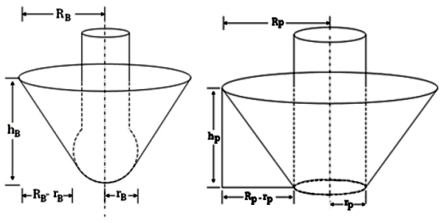

(a) (b)

Fig. 4. Theoretical deformation geometry of the tested fabrics: (a) at the bursting and (b) at the puncture.

TABLE I
CONSIDERED INDEPENDENT VARIABLES

Characteristic	Variable	Level 1	Level 2	Level 3	Level 4	Level 5
*Areal weight (g/m^2) [CV%]	X_1	446 (A) [7.4]	507 (B) [6.6]	544 (C) [6.8]	621 (D) [5.2]	690 (E) [4.3]
Needle penetration depth (mm)	X_2	10	12	14	-	-
Punch density ($1/cm^2$)	X_3	100	150	200	250	300

*Average areal weight of the tested samples in each level+coefficient of variation

TABLE II
TESTED SAMPLES

Code	Areal weight (g/m^2)	Penetration depth (mm)	Punch density ($1/cm^2$)	Code	Areal weight (g/m^2)	Penetration depth (mm)	Punch density ($1/cm^2$)	Code	Areal weight (g/m^2)	Penetration depth (mm)	Punch density ($1/cm^2$)
A1	446	10	100	B11	507	14	100	D6	621	12	100
A2	446	10	150	B12	507	14	150	D7	621	12	150
A3	446	10	200	B13	507	14	200	D8	621	12	200
A4	446	10	250	B14	507	14	250	D9	621	12	250
A5	446	10	300	B15	507	14	300	D10	621	12	300
A6	446	12	100	C1	544	10	100	D11	621	14	100
A7	446	12	150	C2	544	10	150	D12	621	14	150
A8	446	12	200	C3	544	10	200	D13	621	14	200
A9	446	12	250	C4	544	10	250	D14	621	14	250
A10	446	12	300	C5	544	10	300	D15	621	14	300
A11	446	14	100	C6	544	12	100	E1	690	10	100
A12	446	14	150	C7	544	12	150	E2	690	10	150
A13	446	14	200	C8	544	12	200	E3	690	10	200
A14	446	14	250	C9	544	12	250	E4	690	10	250
A15	446	14	300	C10	544	12	300	E5	690	10	300
B1	507	10	100	C11	544	14	100	E6	690	12	100
B2	507	10	150	C12	544	14	150	E7	690	12	150
B3	507	10	200	C13	544	14	200	E8	690	12	200
B4	507	10	250	C14	544	14	250	E9	690	12	250
B5	507	10	300	C15	544	14	300	E10	690	12	300
B6	507	12	100	D1	621	10	100	E11	690	14	100
B7	507	12	150	D2	621	10	150	E12	690	14	150
B8	507	12	200	D3	621	10	200	E13	690	14	200
B9	507	12	250	D4	621	10	250	E14	690	14	250
B10	507	12	300	D5	621	10	300	E15	690	14	300

(BS), bursting real elongation (BRE), puncture resistance (PR) and puncture real elongation (PRE) coded as Y_1 to Y_4, respectively.

III. RESULTS AND DISCUSSION

A. Compressive Behavior Study

The bursting and puncture deformations, respectively, take place while the steel ball and steel plunger compress the tested fabric to the quasi-Gaussian and quasi-hyperbolic statuses which will be finally resulted to fabric rupture.

It is obvious that the results can be obtained in the both states of force-deflection curves and response variables values. The experimental curves show approximately similar behavior, so that four distinguished regions can be considered through the path tracing of the curves. Fig. 5 shows the regions of AB to DE.

The AB region of the compressive curves is related to

the lost thickness of the sample due to going out air from the fabric pores. Then, regarding to more compression during the BC region, a remarkable elongation, but with a slight slope happens. Of course, curve gradient of this region is more than what was happened in the previous region. This can be arisen by fiber crimp opening in fabric structure and consequently more easiness of inter-fibrous displacements. In the CD, gradient of the curve considerably increases. This is due to too much enlargement of contact surface of the compressed fibers. Therefore, this results in an intense increase in fiber to fiber friction which finally, takes place the self-locking phenomenon. It causes to higher resistance of the fabric during deformation. Continuing of this process leads to maximum bursting or puncture compression loading exerted on the fabric which can be conducted to fabric rupture during the DE region. It is clear that both phenomena of fiber slippage and fiber breaking can vividly affect the fabric rupture.

Self-locking point of the compression load-deflection curve can practically defined as transition point between low and high compression modulus regions; where, fibers of consolidated structure of fabric reach a maximum own-entangler condition. In the other word, it tightly increases cohesion-based contact surface of the fibers. Therefore, this can be clearly led to more fiber to fiber entanglement. Fig. 5 shows typical bursting and puncture curves with four distinguished regions. It can be used for description

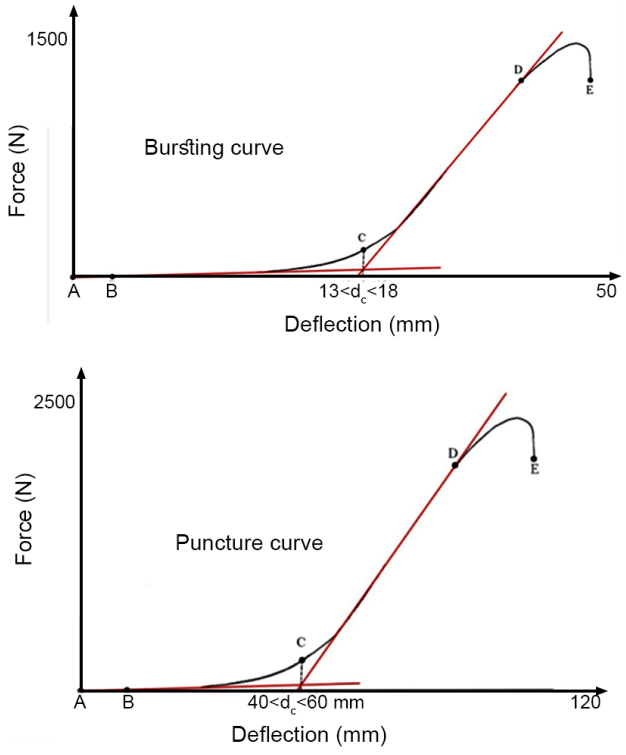

Fig. 5. Typical bursting and puncture curves.

of inherent difference between self-locking conditions in bursting and puncture. Comparison of both compression behaviors in Fig. 5 strongly denotes that the average deflection magnitude of the critical transition points in the studied cases of bursting and puncture are 15 mm and 50 mm, respectively.

Based on the Eqs. (1) and (2), elongation value in transition point of the bursting is calculated 33.84% versus 27.61% of this amount in puncture. This means that the self-locking position for the puncture takes place in less magnitude of elongation in comparison to the similar position of bursting. This is due to the fact that the fibers located under cross section of the puncture's plunger endure stress concentration which is clearly result of the special geometry of the plunger. It is also evident that the spherical shape of the bursting device does not create a considerable and effective stress concentration. Therefore, more fiber displacement in bursting is resulted to more elongation of the fabric before reaching the self-locking situation. In the other word, although the self-locking phenomenon is an undeniable fact in both bursting and puncture behaviors, but the special shape of the bursting device delays the necessary elongation to reach self-locking.

As previously noted, the self-locking condition is resulted by the maximum fiber entanglement which is due to existing contact stress. Therefore, more friction resistance and also shear stress exerted on the fiber bundle can be concluded. Additionally, the fabric rupture can be strongly affected by fiber breakage and also slippage. Stress concentration in puncture causes that the fabric rupture was due to fiber breakage rather than its slippage. Whereas, the bursting ruptures of the fabric is further the result of fiber slippage. This is clearly due to geometry of ball-shaped device which is led to the relative uniformity of the quality of bursting loading. Therefore, more fabric resistance in puncture can be expected.

B. Statistical Analysis

Table III shows mean values of the studied response variables. In order to evaluate statistical significance of the variables, the three-factor factorial design of experiment was used. As emphasized before, changes in studied independent variables were at 5 levels for areal weight, 3 levels for needle penetration depth and 5 levels for punch density. Then, the multivariate regression method was also employed to evaluate the data.

A serious problem that may dramatically influence the usefulness of a regression model is multicollinearity or near-linear dependence among the regression variables. The multicollinearity can seriously affect the precision with which regression coefficients are estimated.

TABLE III
BURSTING AND PUNCTURE RESULTS OF THE TESTED FABRICS*

Code	BS (N) (Y_1)	BRE (%) (Y_2)	PR (N) (Y_3)	PRE (%) (Y_4)	Code	BS (N) (Y_1)	BRE (%) (Y_2)	PR (N) (Y_3)	PRE (%) (Y_4)	Code	BS (N) (Y_1)	BRE (%) (Y_2)	PR (N) (Y_3)	PRE (%) (Y_4)
A1	924.18 (6.51)	121.14 (4.95)	1644.94 (5.82)	91.65 (3.98)	B11	749.13 (13.53)	98.52 (7.52)	1735.60 (11.05)	74.30 (3.64)	D6	1212.79 (10.81)	99.78 (2.92)	2461.75 (0.61)	76.80 (5.44)
A2	827.03 (4.22)	119.92 (6.32)	1298.45 (11.22)	89.76 (2.84)	B12	860.66 (6.96)	93.31 (7.61)	1867.87 (10.66)	61.44 (13.79)	D7	1247.73 (6.07)	86.81 (4.55)	2469.02 (0.53)	76.29 (4.03)
A3	894.50 (5.56)	109.43 (4.81)	1389.52 (11.34)	92.73 (3.78)	B13	956.08 (10.62)	84.62 (2.51)	1343.23 (7.31)	65.82 (1.89)	D8	1231.69 (12.63)	85.24 (6.36)	2234.85 (2.65)	75.85 (2.17)
A4	973.73 (13.14)	111.91 (3.96)	1281.57 (17.45)	83.73 (8.92)	B14	839.20 (7.67)	83.49 (5.75)	1278.59 (12.29)	62.72 (5.49)	D9	1136.52 (18.01)	88.76 (5.65)	2273.47 (8.45)	74.12 (3.66)
A5	822.60 (9.22)	109.24 (1.59)	1349.00 (11.64)	80.95 (3.55)	B15	613.43 (9.52)	95.31 (8.05)	1222.05 (8.98)	75.09 (2.17)	D10	1101.17 (4.33)	97.62 (2.09)	2096.45 (12.75)	78.77 (3.31)
A6	862.30 (13.26)	106.97 (6.75)	1420.22 (13.3)	82.66 (6.71)	C1	1130.82 (16.10)	109.88 (5.46)	2153.53 (6.4)	90.85 (8.33)	D11	1144.11 (11.53)	92.97 (6.48)	2263.87 (7.35)	69.89 (3.11)
A7	826.21 (8.66)	103.95 (1.44)	1529.32 (10.87)	77.31 (4.45)	C2	1100.30 (8.27)	97.48 (3.98)	1576.52 (15.26)	92.84 (2.74)	D12	1218.85 (18.67)	84.43 (7.43)	2150.47 (7.48)	68.91 (4.92)
A8	711.14 (8.93)	96.64 (6.07)	1496.40 (19.83)	84.95 (2.01)	C3	1056.30 (13.71)	118.14 (5.52)	1580.45 (8.49)	94.05 (3.77)	D13	1186.27 (6.96)	80.25 (5.40)	1893.49 (5.87)	62.71 (5.24)
A9	715.26 (9.08)	95.20 (4.66)	1455.85 (7.54)	79.06 (3.62)	C4	1043.64 (12.71)	97.77 (5.80)	1709.62 (5.87)	86.70 (5.64)	D14	1005.83 (5.14)	77.47 (6.99)	1744.17 (8.75)	64.06 (4.96)
A10	785.56 (9.13)	102.06 (3.55)	1407.80 (10.63)	71.31 (3.98)	C5	928.13 (9.90)	107.06 (5.44)	1842.05 (9.64)	89.45 (2.94)	D15	1126.16 (9.85)	91.80 (5.12)	1678.18 (12.05)	57.87 (10.60)
A11	789.88 (8.84)	103.01 (6.31)	1596.42 (6.51)	73.71 (3.03)	C6	971.20 (8.01)	98.77 (3.69)	1872.47 (5.67)	83.99 (2.50)	E1	1446.13 (14.50)	106.30 (9.75)	2561.59 (7.72)	81.82 (11.33)
A12	766.38 (14.44)	91.64 (6.29)	1647.22 (8.82)	69.78 (5.61)	C7	922.82 (18.01)	90.81 (2.14)	1774.62 (12.73)	85.94 (2.78)	E2	1487.16 (15.07)	102.96 (10.85)	2397.27 (5.91)	83.77 (5.16)
A13	727.57 (15.28)	90.76 (7.73)	1036.99 (7.66)	73.46 (4.52)	C8	978.47 (14.51)	90.42 (5.73)	1773.65 (19.81)	83.51 (2.75)	E3	1436.80 (12.93)	96.94 (6.28)	2357.87 (6.14)	79.37 (6.13)
A14	713.58 (17.39)	88.35 (5.87)	1027.22 (6.78)	56.82 (8.59)	C9	927.72 (11.80)	88.75 (4.82)	1860.90 (8.31)	71.42 (6.63)	E4	1357.69 (9.02)	93.94 (5.99)	2475.27 (8.71)	74.78 (6.23)
A15	662.63 (8.69)	92.17 (3.95)	1011.61 (4.72)	68.11 (7.96)	C10	852.11 (8.53)	98.71 (3.27)	1830.75 (4.25)	78.18 (3.03)	E5	1373.40 (3.96)	100.45 (2.67)	2324.35 (7.22)	79.83 (4.91)
B1	937.78 (6.74)	114.66 (2.32)	1933.75 (2.83)	94.08 (4.53)	C11	1050.55 (10.29)	98.73 (4.96)	1755.42 (16.19)	76.19 (5.95)	E6	1370.98 (13.59)	91.46 (3.74)	2370.92 (6.14)	76.56 (4.66)
B2	1038.65 (12.01)	111.26 (3.96)	1496.60 (8.66)	85.41 (4.24)	C12	946.52 (15.55)	85.99 (4.38)	1698.55 (17.49)	76.03 (5.19)	E7	1261.49 (10.87)	91.03 (8.81)	2471.10 (11.89)	76.36 (5.58)
B3	958.79 (11.31)	108.27 (4.30)	1593.37 (10.29)	88.21 (5.12)	C13	843.27 (10.73)	84.71 (5.84)	1644.53 (11.94)	73.45 (4.31)	E8	1199.19 (7.38)	87.13 (4.08)	2422.12 (2.49)	70.18 (3.09)
B4	918.45 (4.42)	109.33 (2.37)	1547.90 (14.34)	83.37 (1.89)	C14	923.96 (12.48)	81.77 (5.86)	1578.71 (10.72)	62.28 (3.10)	E9	1088.78 (12.93)	90.53 (5.39)	2342.35 (5.69)	66.38 (3.10)
B5	1029.92 (7.89)	109.37 (3.18)	1744.95 (18)	78.34 (4.50)	C15	835.26 (6.95)	86.80 (4.79)	1594.82 (12.17)	62.51 (3.07)	E10	1180.50 (6.89)	94.16 (5.65)	2317.45 (4.51)	67.91 (3.86)
B6	904.18 (7.49)	103.52 (3.89)	1386.00 (12.74)	91.06 (3.45)	D1	1221.77 (13.68)	108.96 (7.67)	2578.37 (7.59)	98.35 (6.79)	E11	1308.87 (13.72)	91.48 (5.12)	2326.30 (7.57)	82.51 (2.56)
B7	889.38 (12.65)	95.72 (5.41)	1641.02 (3.27)	78.67 (2.78)	D2	1143.89 (5.95)	97.94 (3.71)	1518.72 (14.79)	90.88 (14.06)	E12	1088.17 (14.77)	84.45 (11.93)	2426.75 (3.52)	60.64 (8.46)
B8	897.40 (8.49)	93.71 (8.19)	1837.57 (14.53)	79.40 (2.93)	D3	1033.08 (8.50)	93.92 (4.63)	1903.02 (3.97)	84.98 (6.75)	E13	1229.18 (5.29)	82.38 (5.28)	2112.51 (7.82)	64.14 (5.14)
B9	807.15 (8.95)	91.27 (2.04)	1761.82 (8.61)	75.17 (5.18)	D4	1168.08 (8.65)	98.85 (3.14)	2143.55 (1.44)	83.84 (1.32)	E14	1264.60 (5.49)	81.29 (2.77)	1944.78 (6.78)	53.82 (4.32)
B10	839.01 (13.24)	99.39 (2.34)	1809.95 (4.83)	68.71 (10.65)	D5	1032.70 (8.60)	100.44 (6.78)	2159.59 (3.70)	82.67 (2.80)	E15	1198.63 (12.13)	89.98 (4.69)	2012.40 (8.71)	58.54 (8.52)

* The amount inside the parenthesis shows coefficient of variation (CV%)

Therefore, variance inflation factors (vifs), as important multicollinearity diagnostic factors, could be used to detect significant influence of the studied variables. In general, the variance inflation factor for the j^{th} regression coefficient can be written as Eq. (3):

$$VIF_j = \frac{1}{1-R_j^2} \quad (3)$$

Where, R^2_j is the coefficient of multiple determinations. The VIF's values larger than 10 imply serious problems with multicollinearity, whereas VIF=1 shows that the analyzed regressors are orthogonal. In this case, the effect of each regressor can be unambiguously determined.

After initial analysis of two essential and major assumptions including normality and constant variance of error, the ANOVA test was carried out. Table IV represents the ANOVA statistical results of the used factorial design. As seen, the analyzed independent variables have high intensity of significance effect on all response variables (P_r<0.0001). On the other hand, the results denoted that there is not any interaction effect between independent variables at their studied levels. Finally, data analysis of the independent variables of fabric areal weight (X_1), needle penetration depth (X_2) and punch density (X_3) were conducted to the equations which can individually predict bursting and puncture behaviors of the nonwoven needle-punched fabrics in various studied attitudes of the independent variables, as shown in Table V. The values of VIF in addition to partial plots also showed that linear relationship between the responses and the regressor variables have been correctly selected.

To evaluate relative importance level of the independent variables, the extra sum of square method was employed. All independent variables were orthogonal and do not multicollinearity with each other due to the fact that the values of Variance Inflation Factor (VIF) are a unit value (Table V). Therefore, using a method accompanied with stepwise selection procedure, the relative importance of independent variables can be achieved individually, as shown in Table VI.

The multi regression results for the bursting strength (Y_1) including P_r<0.0001 and value of R^2 indicate that 87.16% of total studied variations can be predicted by the model. Thereby, the optimal equation of the model can be obtained. Additionally, as shown in Table V, VIF=1 concludes that the partial R^2 of each independent variable can be distinguished individually, i.e. 76.73% of predicted value is affected by the fabric areal weight variable. More fabric areal weight, more bursting strength; whereas increase in both needle penetration depth and punch density

TABLE IV
ANOVA RESULTS OF THE USED FACTORIAL DESIGN OF EXPERIMENT

P_r> F	F-value	Mean square	Sum square	Df	Source	Response variable
<0.0001	210.01	3531545.14	14126180.57	4	X_1	
<0.0001	40.03	673102.57	1346205.15	2	X_2	
<0.0001	9.74	163758.54	655034.14	4	X_3	Y_1
-	-	16816.13	7382281.70	439	Error	
-	-	-	23509701.56	449	Corrected total	
<0.0001	52.14	1890.69	7562.78	4	X_1	
<0.0001	329.79	11958.91	23917.83	2	X_2	
<0.0001	47.73	1730.91	6923.63	4	X_3	Y_2
-	-	36.26	15919.02	439	Error	
-	-	-	54323.16	449	Corrected total	
<0.0001	175.37	8729522.43	34918089.72	4	X_1	
<0.0001	27.66	1376875.93	2753751.86	2	X_2	
<0.0001	13.27	660682.33	2642729.21	4	X_3	Y_3
-	-	49778.53	14385996.09	289	Error	
-	-	-	54700566.99	299	Corrected total	
<0.0001	20.42	629.18	2516.73	4	X_1	
<0.0001	308.80	9513.52	19027.03	2	X_2	
<0.0001	38.43	1183.89	4735.58	4	X_3	Y_4
-	-	30.81	8903.64	289	Error	
-	-	-	35182.98	299	Corrected total	

TABLE V
PARAMETER ESTIMATES FOR THE RESPONSE VARIABLES

VIF	Pr> |t|	t-Value	Standard error	Estimate parameter	Df	Independent variable	Response variable
-	0.0001	4.030	88.223	355.129	1	Intercept	
1	<0.0001	20.600	0.100	2.061	1	X_1	
1	<0.0001	-6.170	5.247	-32.367	1	X_2	Y_1
1	<0.0001	-4.430	0.121	-0.537	1	X_3	
$Y_1=355.129+2.061X_1-32.367\ X_2-0.537X_3$							
-	<0.0001	28.54	6.314	180.20	1	Intercept	
1	<0.0001	-6.34	0.007	-0.045	1	X_1	
1	<0.0001	-11.71	0.375	-4.398	1	X_2	Y_2
1	0.0027	-3.11	0.008	-0.026	1	X_3	
$Y_2= 180.20-0.045\ X_1-4.398X_2-0.026X_3$							
-	0.0173	1.37	226.97	311.73	1	Intercept	
1	<0.0001	15.45	0.26	3.98	1	X_1	
1	0.0044	-2.94	13.49	-39.70	1	X_2	Y_3
1	0.0003	-3.79	0.31	-1.18	1	X_3	
$Y_3=311.73+3.98X_1-39.70\ X_2-1.18X_3$							
-	<0.0001	28.47	5.63	160.39	1	Intercept	
1	0.0001	-4.07	0.006	-0.026	1	X_1	
1	<0.0001	-14.55	0.335	-4.88	1	X_2	Y_4
1	<0.0001	-6.69	0.007	-0.052	1	X_3	
$Y_4=160.39-0.026X_1-4.88X_2-0.052X_3$							

cause that the bursting strength decreases, as indicated in relevant prediction Eq. (Y_1). Enhancement in fabric areal weight (g/m^2) results to further fibers in the cross section of the fabric. This can lead to increase lateral surfaces of burst fibers as well as fiber to fiber friction. As a result, the bursting strength increases. On the other hand, it is evident that vital phenomenon of more fiber breakage due to increase in needle penetration depth and punch density can also vividly conduct nonwoven fabric to experience less bursting strength. Lower value of the bursting strength in higher punch density has been also confirmed by Koç and Çinçik [17].

The bursting elongation was also affected by all three studied independent variables. The value R^2 shows that

TABLE VI
SUMMARY OF STEPWISE SELECTION

P_r> F	F-value	Model R-square	Partial R-square	Independent variable	Step	Response variable
<0.0001	240.66	0.7673	0.7673	X_1	1	
<0.0001	30.22	0.8361	0.0688	X_2	2	Y_1
<0.0001	19.64	0.8716	0.0355	X_3	3	
<0.0001	82.87	0.5317	0.5317	X_2	1	
<0.0001	35.85	0.6874	0.1557	X_1	2	Y_2
0.0027	9.66	0.7248	0.0375	X_3	3	
<0.0001	185.42	0.7175	0.7175	X_1	1	
0.0006	12.97	0.7606	0.0431	X_3	2	Y_3
0.0044	8.65	0.7866	0.0260	X_2	3	
<0.0001	116.85	0.6155	0.6155	X_2	1	
<0.0001	36.76	0.7454	0.1300	X_3	2	Y_4
0.0001	16.60	0.7937	0.0482	X_1	3	

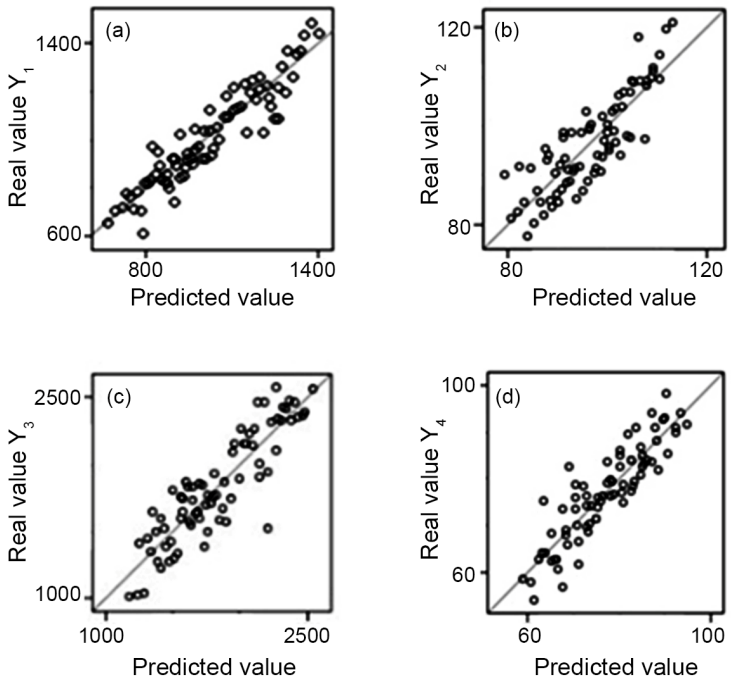

Fig. 6. Predicted versus real values for the response variables.

72.48% of the variations can be predicted by model Y_2. It can be completed by an equation which confirmed that 53.17% of elongation variations is belong to needle penetration depth variable, as shown in Table VI. More magnitude of all studied independent variables not only decreases porosity [15], but also enhances fiber to fiber frictional force. Therefore, it causes that the fibers entanglements which do not permit their displacements to increase. Thereby, less elongation value of the bursting is expectable.

The multi regression results for the puncture resistance (Y_3) including $P_r<0.0001$ and value of R^2 indicate that 78.66% of total studied variations can be predicted by the model. Thereby, the final prediction equation of the model can be resulted. Additionally, as shown in Table V, VIF=1 is concluded that the partial R^2 of each independent variable can be distinguished individually, i.e. 71.75% of predicted value is affected by the fabric areal weight variable (Table VI). More fabric areal weight (g/m^2), more puncture resistance; whereas increase in both needle penetration depth and punch density cause that the puncture resistance decreases, as indicated in relevant prediction Eq. (Y_3). The reaction of the puncture resistance against changes in different values of the independent studied variables, with identical reasons, is also similar to the behavior of the bursting strength.

The puncture elongation was affected by all three studied independent variables. The value R^2 shows that 79.37% of the variations can be predicted by model Y_4. It can be completed by this fact that 61.55% of deflection variations belong to needle penetration depth variable, as shown in Table VI. Less value of the puncture elongation is also anticipated, while magnitudes of the independent variables are increased. This is due to the same proofs described for the bursting.

In order to determine predictive capability of the obtained models, the plots of predicted versus real values for all response variables are shown in Fig. 6. As emphasized before, the R^2 values are 87.16%, 72.48%, 78.66%, and 79.37% for bursting strength (Y_1), bursting elongation (Y_2), puncture resistance (Y_3), and puncture elongation (Y_4), respectively. The high values of R^2 also show a low error prediction.

IV. CONCLUSION

In this study, in order to investigate bursting and puncture behaviors of nonwoven needle-punched polyester fabrics, a three-factor factorial design was employed to evaluate the effect of independent variables. The studied behaviors showed that the samples have undeniable similarities in the compressive deformation, so that four distinguished regions can be considered through the path tracing of the force-deflection curves. Study of the obtained curves showed that the self-locking position for the puncture takes place in less magnitude of elongation in comparison to the similar position of bursting. This is due to the fact that the

fibers located under cross section of the puncture's plunger endure further stress concentration. Stress concentration in puncture causes that the fabric rupture became due to fiber breakage rather than its slippage.

Statistical analysis displayed that all of the studied independent variables are significantly effective on the response variables. The estimator model also indicated that increasing fabric areal weight is resulted to more bursting strength and puncture resistance, whereas it causes to bursting elongation and puncture elongation decrease. This can be due to more fibers in cross section of the fabric and consequently increase in lateral surfaces of burst fibers as well as fiber to fiber friction. The model equations also exhibited that by increasing the needling parameters of punch density and needle penetration depth, the nonwoven fabric shows lower bursting strength and puncture resistance. In addition, more magnitude of needle penetration depth and punch density decreases porosity from one side and it also causes to increase fiber to fiber frictional force from the other side. Thus, the fibers entanglements do not permit their displacements increase. Therefore, it is yielded by less elongation values of bursting and puncture.

REFERENCES

[1] EN ISO 13433, Geosynthetics-Dynamic Perforation Test (Cone Drop Test), 2006.

[2] ASTM D6797-02, Standard Test Method for Bursting Strength of Fabrics Constant-Rate-of-Extension (CRE) ball burst test, 2002.

[3] ISO 12236, International Standard Geosyntetics–Static Puncture Test (CBR test), 2006.

[4] S. Backer and D.R. Petterson, "Some principles of nonwoven fabrics", *Text. Res. J.*, vol. 30, no. 9, pp. 704-711, 1960.

[5] J.W.S. Hearle and A.T. Purdy, "The influence of the depth of needle penetration on needled-fabric structure and tensile", *J. Text. Inst.*, vol. 65, no. 1, pp. 6-12, 1974.

[6] J.W.S. Hearle and M.A.I. Sultan, "A study of needled fabrics part I: experimental methods and properties", *J. Text. Inst.*, vol. 58, no. 6, pp. 251-265, 1967.

[7] J.W.S. Hearle, M.A.I. Sultan, and T.N. Choudhari, "A study of needled fabrics part II: effect of needling process", *J. Text Inst.,* vol. 59, no. 2, pp. 103-116, 1968.

[8] A. Watanabe, M. Miwa, T. Yokoi, and A. Nakayama, "Fatigue behavior of aramid nonwoven fabrics under hot-press conditions part V: effect of punching density on mechanical properties", *Text. Res. J.*, vol. 68, no. 3, pp. 171-178, 1998.

[9] A. Das, R. Alagirusamy, and B. Banerjee, "Study on needle-punched non-woven fabrics made from shrinkable and non-shrinkable acrylic blends. Part I: compressional behavior", *J. Text. Inst.*, vol. 100, no. 1, pp. 10-17, 2009.

[10] S. Debnath and M. Madhusoothanan, "Compression behavior of jute-polypropylene blended needle-punched nonwoven fabrics", *Indian J. Fibre Text. Res.*, vol. 32, no. 4, pp. 427-433, 2007.

[11] S. Debnath and M. Madhusoothanan, "Compression properties of polyester needle-punched fabric", *J. Eng. Fibres Fabr.*, vol. 4, no. 4, pp. 14-19, 2009.

[12] S. Debnath and M. Madhusoothanan, "Compression behavior of jute–polypropylene blended needle-punched nonwoven under wet conditions", *J. Text. Inst.*, vol. 103, no. 6, pp. 583-594, 2012.

[13] A. Rawal, "Effect of dynamic loading on pore size of needle-punched nonwoven geotextiles", *J. Text. Inst.*, vol. 99, no. 1, pp. 9-15, 2008.

[14] A. Rawal, S. Anand, and T. Shah, "Optimization of parameters for the production of needle-punched nonwoven geotextiles", *J. Ind. Text.*, vol. 37, no. 4, pp. 341-356, 2008.

[15] A. Rawal and R. Anandjiwala, "Relationship between process parameters and properties of multifunctional needle-punched geotextiles", *J. Ind. Text.*, vol. 35, no. 4, pp. 271-285, 2006.

[16] T.K. Ghosh, "Puncture resistance of pre-strained geotextiles and its relation to uniaxial tensile strain at failure", *Geotext. Geomembr.*, vol. 16, no. 5, pp. 293-302, 1998.

[17] E. Koç and E. Çinçik, "An investigation on bursting strength of polyester/viscose blended needle-punched nonwovens", *Text. Res. J.*, vol. 82, no. 16, pp. 1621-1634, 2012.

[18] A. Das and R.J. Raghav, "Bursting behavior of spun-bonded nonwoven fabrics: part I- effect of various parameters", *Indian J. Fibre Text. Res.*, vol. 35, no. 3, pp. 258, 2010.

[19] A. Das and R.J. Raghav, "Study on bursting behavior of spun-bonded nonwoven fabrics: part II- change in fabric characteristics dueto repeated bursting cycle", *Indian J. Fibre Text. Res.*, vol. 36, no. 1, pp. 53, 2011.

[20] S. Ghosh and L. Chapman, "Effects of fiber blends and needling parameters on needle-punched moldable nonwoven fabric", *J. Text. Inst.*, vol. 93, no. 1, pp. 75-87, 2002.

[21] Y. Termonia, "Puncture resistance of fibrous structures", *Int. J. Impact Eng.*, vol. 32, no. 9, pp. 1512-1520, 2006.

[22] R. Fangueiro, R. Carvalho, and F. Soutinho, "Mechanical properties of needle-punched nonwovens for geotechnical applications": In: *International Conference on Engineering*, Portugal, 2011.

[23] A.S. Askari, S.S. Najar, and Y.A. Vaghasloo, "Study the effect of test speed and fabric weight on puncture behavior of polyester needle punched nonwoven geotextiles", *J. Eng. Fibers Fabr.*, vol. 7, no. 3, 2012.

[24] T.T. Li, R. Wang, C.W. Lou, J.Y. Lin, and J.H. Lin, "Static and dynamic puncture failure behaviors of 3D needle-punched compound fabric based on weibull distribution", *Text. Res. J.*, vol. 84, no. 18, pp. 1903-1914, 2014.

[25] J.H. Lin, T.T. Li, and C.W. Lou, "Puncture-resisting, sound-absorbing and thermal-insulating properties of polypropylene-selvages reinforced composite nonwovens", *J. Ind. Text.*, vol. 45, no. 6, pp. 1477-1489, 2014.

[26] T.T. Li, R. Wang, C.W. Lou, C.H. Huang, and J.H. Lin, "Mechanical and physical properties of puncture-resistance plank made of recycled selvages", *Fibers Polym.*, vol. 14, no. 2, pp. 258-265, 2013.

[27] T.T. Li, R. Wang, C.W. Lou, and J.H. Lin, "Evaluation of high-modulus, puncture-resistance composite nonwoven fabrics by response surface methodology", *J. Ind. Text.*, vol. 43, no. 2, pp. 247-263, 2013.

[28] T.T. Li, R. Wang, C.W. Lou, and J.H. Lin, "Static and dynamic puncture behaviors of compound fabrics with recycled high-performance Kevlar fibers", *Compos. Part B: Eng.*, vol. 59, pp. 60-66, 2014.

[29] T.T. Li, C.W. Lou, M.C. Lin, and J.H. Lin, "Processing technique and performance evaluation of high-modulus organic/inorganic puncture-resisting composites", *Fiber Text. East. Eur.*, vol. 22, no. 6, pp. 75-80, 2014.

[30] GROZ-BECKERT. Needles; General Catalogue. Germany: GROZ-BECKERT, 2009.